J. Phys. B: At. Mol. Opt. Phys. **32** (1999) 4753–4762. Printed in the UK PII: S0953-4075(99)04057-2

An *ab initio* calculation of electron impact vibrational excitation of NO^+

Ismanuel Rabadán† and Jonathan Tennyson

Department of Physics and Astronomy, University College London, Gower Street, London WC1E 6BT, UK

E-mail: j.tennyson@ucl.ac.uk

Received 6 May 1999, in final form 18 July 1999

Abstract. An *ab initio* calculation, using the *R*-matrix method, of the cross sections for the electron impact vibrational excitation of $NO^+(X\,^1\Sigma^+, v = 0)$ up to $v = 5$ is presented. Calculations have been carried out in both an adiabatic and a non-adiabatic approximation. It is shown that these two approximations produce dramatically different results. This is due to the effect of low-lying Feshbach resonances which can only be treated correctly using the non-adiabatic approach. Rates for vibrational excitation are also presented.

1. Introduction

The one-electron continuum of NO has been the subject of many theoretical and experimental studies. Most of these studies have been carried out from the perspective of ionization of bound states. However, it is also possible to approach this problem from the point of view of collisions which opens up possibilities inaccessible from an ionization perspective. In this approach, one can not only study diffuse bound states of the system, but also electron impact rotational, vibrational and electronic excitation processes (and combinations) of the NO^+ core, as well as the width and position of any quasi-bound resonance states involved.

In previous work we have studied electron impact electronic (Rabadán and Tennyson 1996) and rotational (Rabadán *et al* 1998) excitation of NO^+. In this work we concentrate on the study of vibrational excitation of $NO^+(X\,^1\Sigma^+)$ by electron impact.

Electron impact vibrational excitation of molecular ions can be crucial in determining the population balance of the ions in cool plasmas such as the Earth's ionosphere or the interstellar medium. However, there are essentially no experimental data on this process and only rather limited theoretical work. In particular, as for electron impact rotational excitation, cross sections based on the Coulomb–Born approximation cannot be regarded as reliable (Sarpal and Tennyson 1993, Rabadán *et al* 1998).

The most detailed previous study of electron impact vibrational excitation for a molecular ion, and the only one to consider non-adiabatic effects in the nuclear motion, focused on HeH^+ (Sarpal *et al* 1991b). This work found that while including non-adiabatic effects led to a very complicated structure in the cross sections due to resonances, these effects did not significantly alter the average cross section and hence the rates for electron impact vibrational excitation.

† Present address: Departamento de Química, Universidad Autónoma de Madrid, 28049, Madrid, Spain.

0953-4075/99/194753+10$30.00

The resonance structure in NO is more complicated than in HeH. In this work we study electron impact excitation from the ground vibrational state up to $v = 5$. The study is carried out over a range of energies between 0 and 2.5 eV for the projectile electron. Within the **R**-matrix method, two models for the nuclear motion are explored: an adiabatic calculation and a non-adiabatic one. In the adiabatic calculation the nuclear motion is introduced via a vibrational average of the **T**-matrices obtained with fixed-geometry calculations (Chase 1956). In the non-adiabatic approach, a new **T**-matrix is obtained using a Hamiltonian that includes the nuclear kinetic energy operator, thus going beyond the Born–Oppenheimer approximation (Schneider *et al* 1979). In the non-adiabatic approach, nuclear excited states contribute to the collision which means that the infinite (in principle) series of Rydberg states are included in the calculation. As will be shown below, results in both approximations are dramatically different and the inclusion of non-adiabatic effects in the target excitation process is found to be crucial for the computation of both accurate vibrational cross sections and rates.

2. Theory

2.1. Electron impact calculations

The starting point for these calculations is the fixed-geometry **R**-matrices obtained in Rabadán and Tennyson (1997) (paper I hereafter). The electronic **R**-matrix was taken as a sphere of radius $a = 15\ a_0$ centred on the centre of mass of the molecule. Within this sphere, the wavefunction was obtained using a close-coupling expansion that includes 12 NO^+ target states with wavefunctions represented using configuration-interaction (CI) expansions and (60σ, 57π, 54δ) continuum functions. In addition, L^2 terms were used to account for correlation and orthogonality relaxing effects. Full details on the construction of these target, continuum and system wavefunctions can be found in paper I.

These inner region **R**-matrix calculations were repeated at 14 internuclear separations from $R = 1.606$ to $2.835\ a_0$. These calculations gave the **R**-matrix poles as a function of R used in the non-adiabatic model. For the adiabatic model, **T**-matrices were obtained for each geometry by solving the outer region problem as a function of energy. As before, we found that retaining only channels associated with the NO^+ ground state in the outer region calculation led to large savings in computer time with negligible loss of accuracy at the low energies of interest here.

2.2. Adiabatic model

In the adiabatic model, the **T**-matrices, as a function of R, are vibrationally averaged using vibrational functions obtained in the ground state potential energy curve of NO^+. According to Chase (1956):

$$ {}^{\mathrm{A}}T^{\Lambda}_{l'v',lv} = \int \chi_{v'}(R)\, {}^{\mathrm{FN}}T^{\Lambda}_{l',l}(R)\, \chi_v(R)\, \mathrm{d}R \tag{1} $$

where the vibrational wavefunctions of the target, χ_v, were obtained using the program LEVEL (LeRoy 1996) which solves the radial Schrödinger equation numerically. For this we used the *ab initio* $NO^+(X\ ^1\Sigma^+)$ potential of paper I.

2.3. Non-adiabatic model

We use the non-adiabatic **R**-matrix implementation (Gillan *et al* 1987) of the corresponding approximation introduced by Schneider *et al* (1979).

As in the fixed-nuclei **R**-matrix method, configuration space is partitioned in two regions. The internal region is the hypersphere defined by $0 \leqslant r \leqslant a$ and $A_{\text{in}} \leqslant R \leqslant A_{\text{out}}$, where r is the electronic coordinate and R the internuclear distance. As above, we take $a = 15\,a_0$. For the nuclear motion we use $A_{\text{in}} = 1.606\,a_0$ and $A_{\text{out}} = 2.835\,a_0$, this spans a big enough region that vibrational functions with $v \leqslant 5$ can safely be assumed to have negligible amplitude outside this range.

In the internal region, the Hamiltonian ($\mathcal{H}$) includes the nuclear kinetic energy operator (T_R), the electronic Hamiltonian of the $N + 1$ system (H_{N+1}) and the Bloch operator (L_{N+1}) to ensure Hermiticity. This Hamiltonian is diagonalized in a basis set $\{\theta_k\}$ built as

$$\theta_k = \sum_{ij} \Psi_i(R_0)\,\xi_j(R)\gamma_{ijk} \tag{2}$$

where Ψ_i is the fixed-nuclei electronic wavefunction given in paper I and ξ_j is a set of Legendre polynomials, 75 in this work, used to describe the nuclear motion. This basis is diabatic because it does not diagonalize H_{N+1} (except at $R = R_0 = 1.606\,a_0$), but has the advantage of commuting with T_R, and this greatly simplifies the diagonalization of $\mathcal{H}$.

In the external region, the wavefunction is expanded as

$$\theta = \sum_{iv} \phi_i r_{N+1}^{-1} F_{iv}(r_{N+1}) Y_{l_i m_i}(\hat{\boldsymbol{r}}_{N+1})\chi_{iv}(R) \tag{3}$$

where ϕ_i are the target electronic wavefunctions, χ_{iv} the target vibrational wavefunctions and F_{iv} mono-electronic radial functions. Target vibrational wavefunctions generated for the adiabatic calculations were employed.

The matching of the internal and external wavefunctions on the hypersphere surface, and the use of the asymptotic boundary conditions for F_{iv}, as in the standard **R**-matrix method, leads to the calculation of the non-adiabatic **T**-matrix. This is then used to obtain the collisional parameters and, in particular, the eigenphase sum.

In practice, only the electronic ground state and 10 vibrational channels are included in equation (3). It was shown in paper I that the use of only one electronic state in the external region produced only very minor differences in the position of the Rydberg states but saves considerable CPU time.

In the non-adiabatic model, the potentials for the nuclear motion are provided by the **R**-matrix poles, i.e. the eigenvalues of the Hamiltonian in the inner region. It is possible to classify these poles as being of several types. At higher energies many of the poles are simply a representation of the continuum which is discretized by the finite size of the **R**-matrix sphere. At energies below that of the target ground state, the poles give a representation of bound states of the compound system. For an ionic target, such as NO^+, the higher of these poles correspond to Rydberg states. Some **R**-matrix poles follow electronically excited states of the target, again giving a representation of Rydberg states converging to the excited target states. In reality such states are usually Feshbach resonances. Finally, there are usually a small number poles which represent excited valence states of the compound system. In the case of NO, these states can change from being autoionizing to being bound as a function of R. As these states cross Rydberg series they are known as intruder, see paper I, or interloper (Ballance *et al* 1998) states.

For NO at low energies there are poles which correspond to Rydberg states of $NO^+(X\,^1\Sigma^+)$, and poles which correspond to valence states, or possibly Rydberg states of NO^+ excited states.

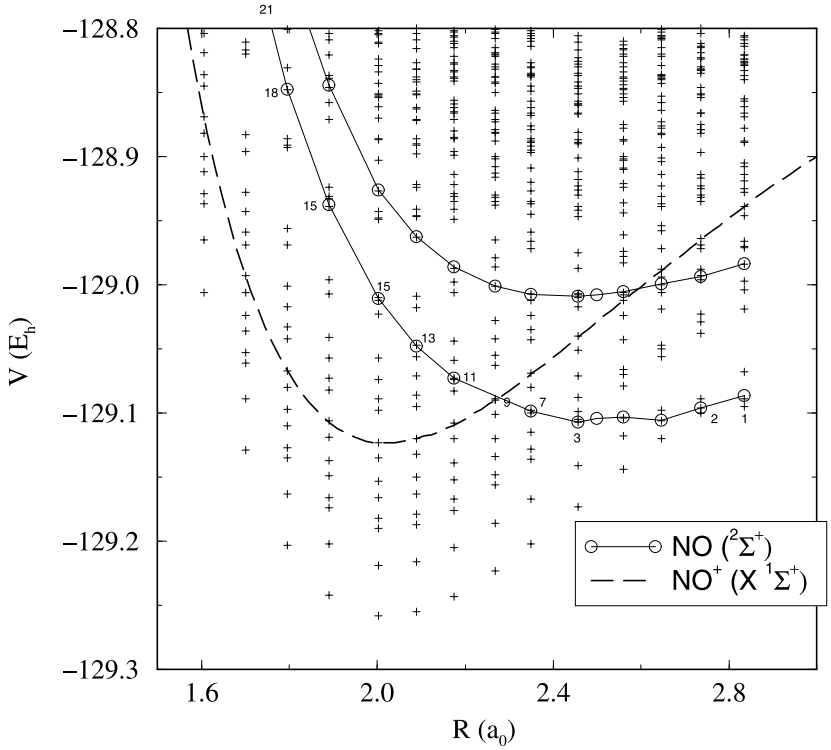

Figure 1. Map of **R**-matrix poles of NO($^2\Sigma^+$). Included are curves for the NO^+ ground state (broken curve) and two NO valence states (full curves). Numbers accompanying the lowest valence state indicate the number of the **R**-matrix pole associated with the state.

These two groups of states show a markedly different behaviour as a function of R. For the non-adiabatic procedure employed here, crossings between these poles as R changes must be correctly identified in the range of energies of interest.

In a model which included full non-adiabatic couplings, the correct identification of individual avoided crossings would not be crucial. However, the present procedure only allows for these couplings approximately, via variation in the CI coefficients, and is therefore sensitive to how the crossings are treated, at least in the energy region of interest.

Figure 1 shows the **R**-matrix pole positions obtained for the symmetry $^2\Sigma^+$. Included in this figure are the positions of the intruder states of NO obtained in paper I. These values help in identifying poles that correspond to these states. This information has been used to specify crossings between poles.

Similarly, figure 2 presents the map of **R**-matrix poles for the $^2\Pi$ symmetry. Here, the crossings of three valence states have been accounted for. Figure 3 shows the corresponding map for **R**-matrix poles of NO($^2\Delta$). Only one valence state had to be specified in this case.

The dissociative 'valence' states depicted in figures 1–3 are the states responsible for dissociative recombination in NO^+ (Sun and Nakamura 1990, Vejby-Christensen *et al* 1998). These curves are being used to study this process, the results of which will be reported in a subsequent paper.

Inspection of figures 1–3 shows that at higher energies the density of **R**-matrix poles becomes very high and any attempt to join these curves diabatically is unlikely to succeed.

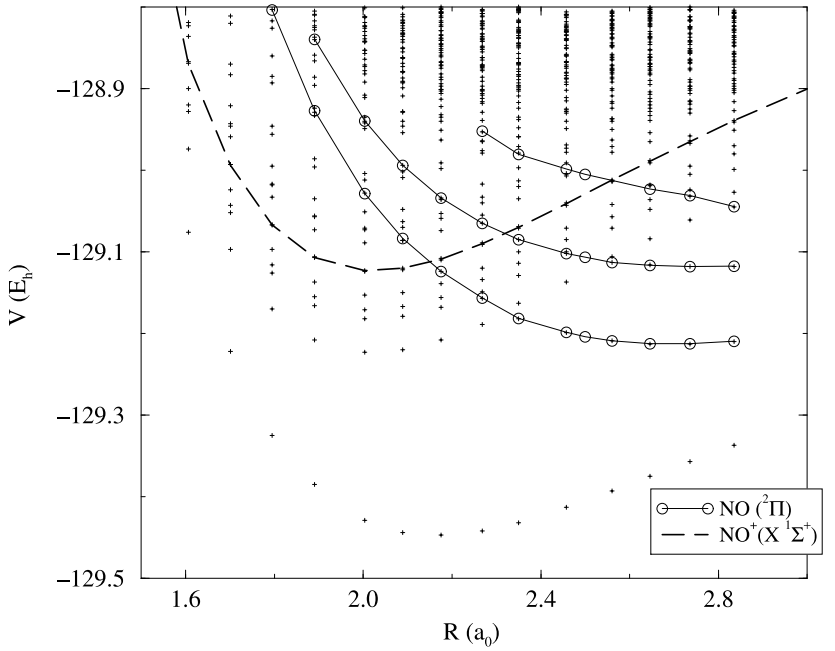

Figure 2. Map of **R**-matrix poles of NO($^2\Pi$). Included are curves for the NO^+ ground state and three NO valence states.

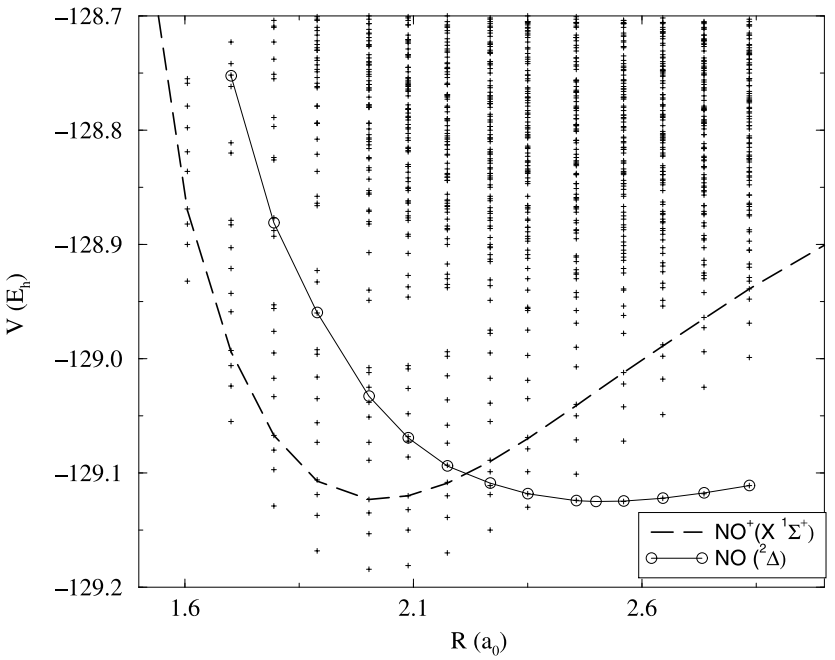

Figure 3. Map of **R**-matrix poles of NO($^2\Delta$). Included are curves for the NO^+ ground state and one NO valence state.

However, the non-adiabatic procedure of Gillan *et al* (1987) treats the higher poles adiabatically and only requires detailed consideration of poles in the energy region of interest and below. For this purpose we used the first 13 for the $^2\Sigma^+$ symmetry calculations, the lowest 16 for the $^2\Pi$ calculations and the lowest 11 for calculations of $^2\Delta$ symmetry. In practice, very similar results should be obtainable with fewer non-adiabatically coupled **R**-matrix poles. Bound state calculations were used to test this model.

3. Results

3.1. Bound state calculations

The specification of pole crossings and pole coupling is quite delicate in the non-adiabatic calculations. The wrong selection can lead to results that are unreliable. To ensure that our choice is consistent, we performed a series of bound state calculations using our scattering wavefunctions (Sarpal *et al* 1991a, Rabadán and Tennyson 1996). The results should be similar to simpler, Born–Oppenheimer, calculations that compute bound vibrational states in the potential energy curves obtained previously, in paper I, using the same model for the electronic structure part of the calculation.

Table 1. Comparison between the energy (in Hartrees) of the first 10 vibrational states of NO(X $^2\Pi$) and NO(A $^2\Sigma^+$) obtained with the non-adiabatic method and Born–Oppenheimer (BO) results obtained by numerical integration of the potential energy curves.

	NO(X $^2\Pi$)		NO(A $^2\Sigma^+$)	
v	Non-adiabatic	BO	Non-adiabatic	BO
0		−129.4433	−129.2526	−129.2528
1	−129.4342	−129.4344	−129.2419	−129.2422
2	−129.4252	−129.4252	−129.2313	−129.2316
3		−129.4163	−129.2209	−129.2212
4	−129.4073	−129.4077	−129.2106	−129.2110
5	−129.3987	−129.3992	−129.2014	−129.2009
6	−129.3903	−129.3909	−129.1911	−129.1908
7	−129.3821	−129.3828	−129.1809	−129.1808
8	−129.3740	−129.3748	−129.1711	−129.1711
9	−129.3662	−129.3670	−129.1615	−129.1615

An example of the bound states calculations carried out with the model of pole-crossing chosen is shown in table 1 for the X $^2\Pi$ and A $^2\Sigma^+$ states of NO. The table compares results obtained with the non-adiabatic model, which gives vibrational energies directly, and vibrational states obtained in the potential energy curves. The agreement between both models is very good. This proves two points: that the model chosen for the non-adiabatic calculation is correct and that the non-adiabatic (non Born–Oppenheimer) effects on the bound states are of little importance, as is generally assumed.

There is a subtle difference between the Born–Oppenheimer procedure used to obtain the bound states, and the adiabatic nuclei model discussed in section 2.2 above. Both methods are usually regarded as being based on the Born–Oppenheimer approximation, but differ in the potential energy curves used to solve the nuclear motion problem. The bound states were obtained using the curves for NO, while the vibrational excitation model uses NO^+ ion curves and associated vibrational wavefunctions.

3.2. Vibrational excitation

We have performed a series of electron impact vibrational excitation calculations using both the adiabatic and non-adiabatic models. Typical results are given in figure 4 for $v = 0 \rightarrow 1$ excitations. It is clear that the two models give radically different results.

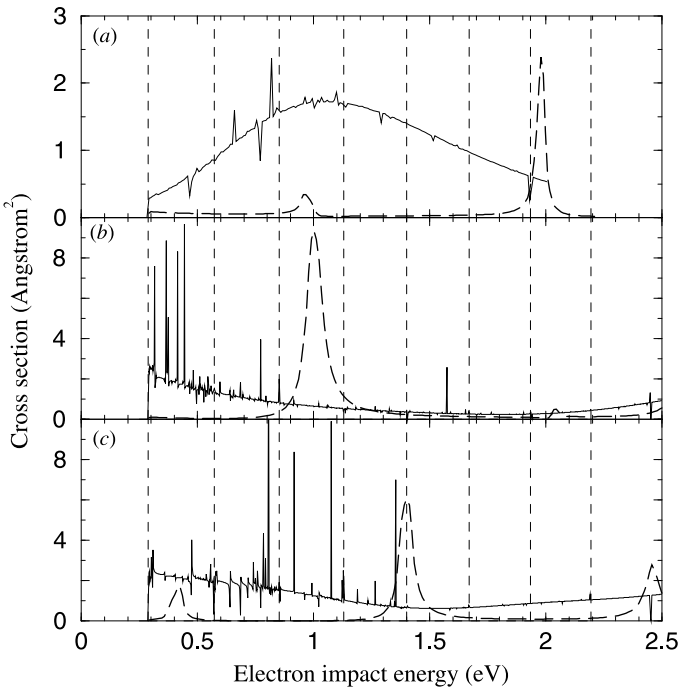

Figure 4. Electron impact vibrational excitation cross sections for $NO^+(X\,^1\Sigma^+, v = 0 \rightarrow 1)$ calculated with the non-adiabatic (full curve) and adiabatic (long-broken curve) models. (*a*) $^2\Sigma^+$, (*b*) $^2\Pi$ and (*c*) $^2\Delta$ total symmetry calculations. Vibrational thresholds are indicated by vertical broken lines.

The adiabatic nuclei calculations give very low cross sections except for a few isolated, broad resonances. These resonance features are the consequence of the many low-lying Feshbach resonances present in the NO system, both those which correlate with excited electronic states of NO^+ and the intruder states depicted in figures 1–3 above. The adiabatic nuclei approximation is not appropriate for these long-lived resonances states as, when the system is trapped in a resonance state, the nuclei move on the NO resonance curve rather than the NO^+ curve used to generate the target wavefunctions. To treat this situation it is therefore necessary to move beyond the adiabatic nuclei approximation.

The non-adiabatic calculations treat these resonances and introduce another set of resonances into the problem. These second set of resonances correspond to vibrationally excited states of high-lying Rydberg states converging to the NO^+ X $^2\Pi$ ground state. Such resonances are known as nuclear excited Feshbach resonances and are particularly long lived. They are responsible for the very narrow resonant features that appear in the non-adiabatic cross sections. Their narrowness means that they contribute a relatively small amount to the average cross section.

In contrast the Feshbach resonances lead to a significant increase in the vibrational

excitation cross sections. That vibrational excitation cross sections for neutral targets are dominated by resonances is well known (Morrison and Sun 1995). The difference here is that the many resonances, and in particular the intruder states, mean that there are potential resonances essentially at all electron impact energies. This leads to significant vibrational excitation cross sections over the whole energy range considered here.

Figure 5 gives electron impact vibrational excitation cross sections from the NO^+ vibrational ground states to the lowest five vibrationally excited states. All results are for a non-adiabatic calculation. Total cross sections were obtained by summing $^2\Sigma^+$, $^2\Pi$ and $^2\Delta$ symmetries, as our previous studies have shown that higher symmetries make a negligible contribution. As might have been anticipated, the largest cross sections were obtained for the $v = 0 \rightarrow 1$ transition. This cross section is a factor of about ten smaller than the highest rotational excitation cross section, the $j = 0 \rightarrow 2$ given by the calculations of Rabadán *et al* (1998).

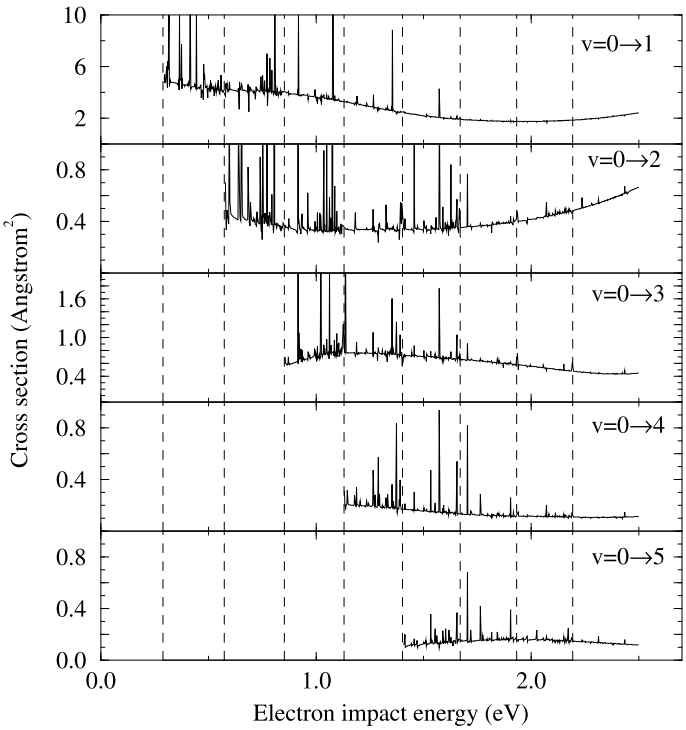

Figure 5. Total electron impact vibrational excitation cross sections of $NO^+(X\,^1\Sigma^+)$ computed using the non-adiabatic model. Vibrational thresholds are indicated by vertical broken lines.

Electron impact vibrational excitation of NO^+ could be an important process in a number of environments, including the Earth's upper atmosphere. We have therefore used the cross sections depicted in figure 5 to compute excitation rates as a function of electron temperature, assuming a Maxwellian distribution for the electron velocities. Figure 6 shows the rate of vibrational excitation calculated using the non-adiabatic cross section for these processes. In these calculations, explicit cross sections were used up to 2.5 eV. Estimation of the high-energy tail using constant cross sections above this energy suggests that the error in the rates at 10 000 K is between 15 and 40%, while below 5000 K the error is smaller

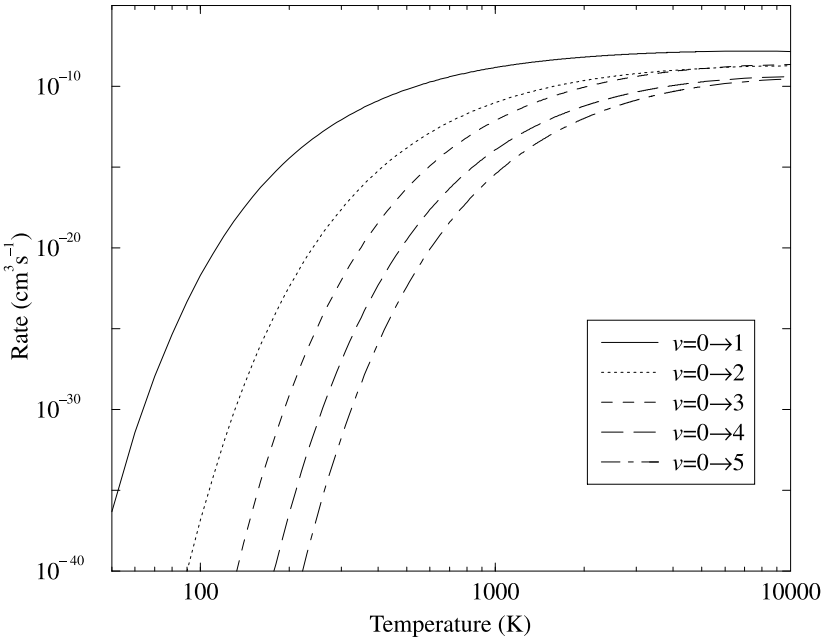

Figure 6. Non-adiabatic rates for the excitation of $NO^+(X\ ^1\Sigma^+, v = 0)$ to the first five vibrational levels.

than 10%.

4. Conclusions

Electron impact vibrational excitation cross sections have been computed for the molecular ion NO^+ using a double **R**-matrix procedure. In contrast to the only previous detailed study of this process for a molecular ion which focused on HeH^+ (Sarpal *et al* 1991b), we find that both the cross sections and rates are sensitive to the level of theory used to treat the nuclear motion in the problem. Significantly larger cross sections are obtained using a non-adiabatic rather than an adiabatic treatment of the vibrational coordinate. This difference can be ascribed to the large number of low-lying Feshbach resonances in the electron–NO^+ problem. Such resonances are absent from the equivalent electron–HeH^+, explaining the difference in behaviour between the two systems. The HeH system is rather unusual in that it does not possess low-lying autoionizing states. It is to be expected that to obtain reliable results for electron impact vibrational excitation for most molecular ions, the process will have to be studied using a non-adiabatic treatment.

Acknowledgments

We thank Lesley Morgan for helpful discussions during the course of this work. This work was supported by the UK Engineering and Physical Sciences Research Council under grants GR/K47702 and GR/K89214.

References

Ballance C P, McLaughlin B M and Berrington K A 1998 *J. Phys. B: At. Mol. Opt. Phys.* **31** L655–65
Chase D M 1956 *Phys. Rev.* **104** 838–42
Gillan C J, Nagy O, Burke P G, Morgan L A and Noble C J 1987 *J. Phys. B: At. Mol. Phys.* **20** 4585–603
LeRoy R J 1996 *University of Waterloo Chemical Physics Research Report* **CP-555R** 1–11
Morrison M A and Sun W 1995 *Computational Methods for Electron Molecule Collisions* (New York: Plenum) pp 131–90
Rabadán I, Sarpal B K and Tennyson J 1998 *J. Phys. B: At. Mol. Opt. Phys.* **31** 2077–90
Rabadán I and Tennyson J 1996 *J. Phys. B: At. Mol. Opt. Phys.* **29** 3747–61
——1997 *J. Phys. B: At. Mol. Opt. Phys.* **30** 1975–88
Sarpal B K, Branchett S E, Tennyson J and Morgan L A 1991a *J. Phys. B: At. Mol. Opt. Phys.* **24** 3685–99
Sarpal B K and Tennyson J 1993 *Mon. Not. R. Astron. Soc.* **263** 909–12
Sarpal B K, Tennyson J and Morgan L A 1991b *J. Phys. B: At. Mol. Opt. Phys.* **24** 1851–66
Schneider B I, Dourneuf M L and Burke P G 1979 *J. Phys. B: At. Mol. Phys.* **40** L365–9
Sun H and Nakamura H 1990 *J. Chem. Phys.* **93** 6491–501
Vejby-Christensen L, Kella D, Pedersen H B and Andersen L H 1998 *Phys. Rev.* A **57** 3627–34